The Plant Cell, Vol. 15, 1095–1110, May 2003, www.plantcell.org © 2003 American Society of Plant Biologists

Dominant-Negative Receptor Uncovers Redundancy in the Arabidopsis ERECTA Leucine-Rich Repeat Receptor–Like Kinase Signaling Pathway That Regulates Organ Shape

Elena D. Shpak,[a] Michael B. Lakeman,[a] and Keiko U. Torii[a,b,1]

[a] Department of Biology, University of Washington, Seattle, Washington 98195-1800
[b] CREST, Japan Science and Technology Corporation, Kawaguchi, Saitama 322-0012, Japan

Arabidopsis ERECTA, a Leu-rich repeat receptor-like Ser/Thr kinase (LRR-RLK), regulates organ shape and inflorescence architecture. Here, we show that a truncated ERECTA protein that lacks the cytoplasmic kinase domain (ΔKinase) confers dominant-negative effects when expressed under the control of the native *ERECTA* promoter and terminator. Transgenic plants expressing ΔKinase displayed phenotypes, including compact inflorescence and short, blunt siliques, that are characteristic of loss-of-function *erecta* mutant plants. The ΔKinase fragment migrated as a stable ~400-kD protein complex in the complete absence of the endogenous ERECTA protein and significantly exaggerated the growth defects of the null *erecta* plants. A functional LRR domain of ΔKinase was required for dominant-negative effects. Accumulation of ΔKinase did not interfere with another LRR-RLK signaling pathway (CLAVATA1), which operates in the same cells as ERECTA but has a distinct biological function. Both the *erecta* mutation and *ΔKinase* expression conferred a lesser number of large, disorganized, and expanded cortex cells, which are associated with an increased level of somatic endoploidy. These findings suggest that functionally redundant RLK signaling pathways, including ERECTA, are required to fine-tune the proliferation and growth of cells in the same tissue type during Arabidopsis organogenesis.

INTRODUCTION

The bodies of higher plants are built by a reiterative formation of the shoot system, which consists of a node bearing a lateral organ (e.g., a leaf) and an internode (e.g., a stem). Both lateral organs and internodes are generated from distinct domains of the shoot apical meristem, in which continual cell proliferation and differentiation take place. The basic pattern and identity of the shoots are determined at the shoot apical meristem, and their final size and shape, which contribute to the diversity of the plant form, are elaborated by localized cell division and cell expansion during plant organ morphogenesis.

Although mechanisms for plant cell division and expansion have been studied extensively, little is known about how these two cellular processes are integrated in the context of whole plant growth and development. Transgenic studies of cell cycle regulators revealed intimate crosstalk between these two processes. For instance, transgenic tobacco plants overexpressing a dominant-negative form of Cdc2 produced nearly normal organs, both in overall size and patterning, despite the fact that the transgene severely compromised cell division (Trotochaud et al., 1999). Although overexpression of the cyclin kinase inhibitor ICK1 in Arabidopsis plants resulted in small organs, the cells that made up such small organs were much larger than control cells (Wang et al., 2000). These findings imply that plants may somehow monitor and balance the activity of cell division and cell expansion to retain a stable organ size. Therefore, revealing the mechanisms that coordinate these two processes at the supracellular level is critical for a better understanding of plant growth and development.

The molecular basis of the cell-to-cell signaling that coordinates cell division and expansion during plant organogenesis is not clear. One candidate gene is Arabidopsis *ERECTA*, which regulates organ shape and inflorescence architecture. Loss-of-function *erecta* mutations confer a compact inflorescence with short internodes and clustered flower buds, short pedicels, round flowers, and short, blunt siliques (Bowman, 1993; Torii et al., 1996). Despite these defects, the *erecta* mutation does not affect organ identity, polarity, or tissue organization. As such, Landsberg *erecta* has been used widely as a "wild type" because of its preferable, compact plant size. Cellular defects caused by *erecta* are not documented extensively; however, both cell size and number are altered in *erecta* inflorescence stems (Komeda et al., 1998). Consistent with its role in organogenesis, *ERECTA* is expressed at high levels in the entire shoot apical meristem and developing organs (Yokoyama et al., 1998). *ERECTA* encodes a Leu-rich repeat receptor-like kinase (LRR-RLK) with functional Ser/Thr kinase activity (Torii et al., 1996; Lease et al., 2001a). The LRR-RLKs constitute the largest subfamily of plant RLKs and possess a structural organization similar to that of animal receptor kinases (Torii, 2000; Shiu and Bleecker, 2001). Several LRR-RLKs function as important developmental regulators, including Arabidopsis CLAVATA1 (CLV1), which balances cell proliferation and differentiation in the meristem, RLK5/HAESA, which promotes flower abscission, and

[1] To whom correspondence should be addressed. E-mail ktorii@u.washington.edu; fax 1-206-685-1728.
Article, publication date, and citation information can be found at www.plantcell.org/cgi/doi/10.1105/tpc.010413.

the brassinosteroid (BR) receptor BRI1 (Clark et al., 1997; Li and Chory, 1997; Jinn et al., 2000). The mutant phenotypes, expression patterns, and molecular identity of ERECTA as an LRR-RLK support the notion that ERECTA mediates yet to be identified cell-to-cell signaling pathways that coordinate shoot organ growth.

To understand how ERECTA regulates organ growth, it is essential to elucidate its modes of action as a receptor kinase and to identify other components of the ERECTA-mediated signal transduction pathway. A large-scale genetic screen searching for the erecta phenotype led to the isolation of 16 additional *erecta* alleles but failed to identify novel loci whose mutations confer phenotypes identical to that of *erecta* (Lease et al., 2001a, 2001b). This finding implies that other components of the ERECTA signaling pathway are redundant. Therefore, their mutations may not have an erecta-like phenotype; instead, they may display no phenotype at all, a subset of the erecta phenotypes, more severe phenotypes, or even be lethal. From the same genetic screen, *erecta-like4* (*elk4*) was identified as a silique-specific genetic interactor of *erecta*, suggesting that ELK4 may be a tissue-specific component of the ERECTA signaling pathway (Lease et al., 2001b). *ELK4* encodes AGB1, a putative β-subunit of the heterotrimeric G-proteins, which are known to transduce signals via seven transmembrane G-protein–coupled receptors in animals (Lease et al., 2001b). It remains to be determined how heterotrimeric G-proteins interact with the ERECTA LRR-RLK signaling pathway.

We sought to dissect the ERECTA signaling pathway using a transgenic approach. Expression of truncated receptor kinases has been used widely as a powerful tool to reveal in vivo function and signal transduction of animal receptor kinases. For both animal receptor Tyr kinases (RTK) and transforming growth factor β receptor Ser/Thr kinases, the general consensus is that truncated receptors that lack the cytoplasmic kinase domain act as dominant-negative receptors by blocking the normal activity of the endogenous counterparts (Amaya et al., 1991; Ueno et al., 1991; Hemmati-Brivanlou and Melton, 1992; Freeman, 1996). Such an approach has not been pursued actively in plant RLK studies because of frequent cosuppression events (Conner et al., 1997; Schumacher and Chory, 2000). An additional confusion in understanding the modes of action of the plant RLK is that the kinase domain of LRR-RLK appears dispensable, because truncated mutations that remove the entire kinase domain of two LRR-RLKs, CLV1 and rice Xa21, retain partial activity (Clark et al., 1997; Wang et al., 1998; Torii, 2000).

Here, we report that truncated ERECTA protein that lacks the cytoplasmic kinase domain (ΔKinase) interferes with endogenous ERECTA function. Therefore, unlike CLV1 and Xa21, ΔKinase of ERECTA acts as a dominant-negative receptor. Importantly, the ΔKinase protein enhances the phenotype of the null *erecta* plants. ΔKinase migrates as an ~400-kD protein complex in the absence of the endogenous ERECTA protein, suggesting that ΔKinase associates with other RLKs and/or ligands, which are shared by other RLKs, and blocks their functions. Based on cell biological analysis of the *erecta* mutants and ΔKinase transgenic plants, we propose that multiple overlapping and interrelated RLK signaling pathways, including ERECTA, are required for coordinated cell proliferation and cell growth within the same tissue types during Arabidopsis organogenesis.

RESULTS

Transgenic Plants That Express *ΔKinase* Display the *erecta* Mutant Phenotype

We introduced into Arabidopsis wild-type *ERECTA* plants (ecotype Columbia) a truncated ERECTA that retains the extracellular LRR and transmembrane domains but lacks the cytoplasmic kinase domain (ΔKinase). To ensure the proper temporal/spatial expression patterns of the truncated ERECTA, the 1.7-kb 5′ and 1.9-kb 3′ regions of the Columbia *ERECTA* locus, which correspond to the *ERECTA* promoter and terminator, respectively (Yokoyama et al., 1998), as well as a genomic fragment of *ΔKinase*, which contains all 23 introns (Torii et al., 1996), were used to express *ΔKinase*. The ΔKinase fragment contains a short cytoplasmic tail of 12 amino acids, which is juxtaposed to the putative transmembrane domain. Fifty-one of 54 independent T1 plants showed a phenotype resembling that of loss-of-function *erecta* mutant plants (Figure 1). Analysis of the selfed T2 progeny revealed that the phenotype was dominant and linked tightly to the transgene (data not shown). Among the lines that contained a single T-DNA insertion, two lines (L1 and L2) with strong phenotype and one line (L3) with mild phenotype were chosen for a further characterization.

Transgenic *ERECTA*::*ΔKinase* plants had short stature and developed a compact inflorescence, short pedicels, and short, blunt siliques, all of which are reminiscent of loss-of-function *erecta* mutant plants (Figures 1A to 1D). The *ERECTA*::*ΔKinase* inflorescence tip displayed a characteristic clustering, which was indistinguishable from that of the intermediate allele *erecta-103* (Figure 1B) (Torii et al., 1996). Detailed morphometric analysis revealed that plant height and pedicel length of *ERECTA*::*ΔKinase* plants were intermediate between those of the wild type and the null allele *erecta-105*, with L3 being tallest (Figure 1E). Silique lengths of all three lines were as short as that of *erecta-105* (Figure 1E). The morphology of the silique tips was analyzed in detail (Figure 1C). The tip of the wild-type silique had an elongated style that protruded from narrow valves. By contrast, the tips of the *erecta* and *ERECTA*::*ΔKinase* siliques (L2) had short and broad styles (Figure 1D). These results suggest that the organ elongation defects conferred by *ERECTA*::*ΔKinase* highly resemble the disruption of normal *ERECTA* function. The transgenic plants also displayed reduced fertility as a result of defective elongation of the stamen filaments (data not shown).

Accumulation of the *ΔKinase* Fragment Confers Dominant-Negative Interference

The erecta phenotype conferred by the introduction of *ERECTA*::*ΔKinase* could be attributable to dominant-negative interference of the ERECTA pathway by the truncated ERECTA receptor. Alternatively, it could be the result of the cosuppression of endogenous *ERECTA* gene expression. To distinguish between these two possibilities, we next examined the level of

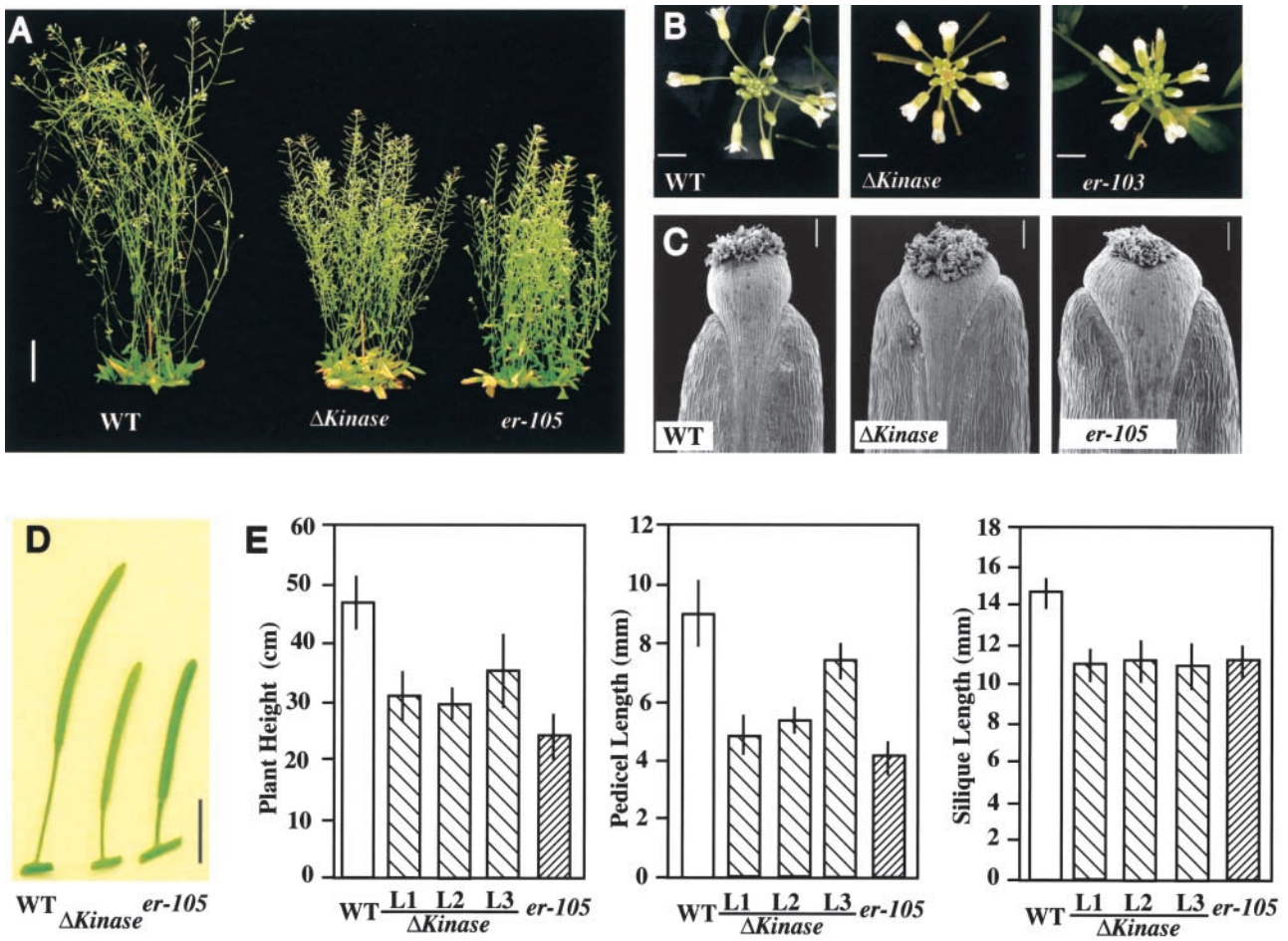

Figure 1. *ERECTA*::*ΔKinase* Confers Dominant-Negative Effects in Arabidopsis Morphology.

(A) Seven-week-old plants of the wild type (WT), *ΔKinase*, and *erecta-105*. Bar = 4 cm.
(B) Inflorescence apices from the wild type, *ΔKinase*, and *erecta-103*. Bars = 3 mm.
(C) Scanning electron micrographs of silique tips from the wild type, *ΔKinase*, and *erecta-105*. Bars = 100 μm.
(D) Siliques and attached pedicels of the wild type, *ΔKinase*, and *erecta-105*. Bar = 5 mm.
(E) Morphometric analysis of fully grown 7-week-old plants of the wild type, *erecta-105*, and three independent transgenic lines (L1, L2, and L3) of *ERECTA*::*ΔKinase*. Twenty-five plants were analyzed for plant (inflorescence) height. Lengths of 50 mature pedicels and siliques on the main inflorescence stem (10 measurements per stem) were analyzed. Bars represent average values ± SD.

the endogenous *ERECTA* transcripts in three transgenic lines. Reverse transcriptase–mediated (RT) PCR analysis using primers that anneal to the kinase domain revealed that levels of the endogenous *ERECTA* transcripts were not altered significantly by the transgene, excluding the possibility of cosuppression (Figure 2A).

From immunoblots probed with antibody raised against the ERECTA LRR domain (anti-ERLRR), endogenous ERECTA was detected as a band of ~145 kD in both wild-type and transgenic plants (Figure 2B). In the *erecta-105* null allele background, we detected a very faint band at a similar position (Figure 2B), likely representing LRR-RLKs closely related to ERECTA. The higher molecular mass of ERECTA compared with its calculated molecular mass (105 kD) suggests a possible glycosylation, because the extracellular domain of ERECTA possesses 12 potential *N*-glycosylation sites (Torii et al., 1996). Several other plant LRR receptors, including tomato Cf-4/Cf-9 and the carrot phytosulfokine receptor, have been shown to be glycosylated (Piedras et al., 2000; Matsubayashi et al., 2002; Rivas et al., 2002a, 2002b). The ΔKinase protein migrates at ~95 kD (the predicted polypeptide is 64 kD) and therefore may be glycosylated as well (Figure 2B).

Interestingly, we found that the ΔKinase protein was accumulated at much higher levels than the full-length, endogenous ERECTA protein (Figure 2B). A quantitative analysis of the immunoblot signals estimated that the amount of ΔKinase was ~100 times greater in L1 and L2 and ~30 times greater in L3 than the endogenous ERECTA (Figure 2B). RT-PCR analysis with primers that amplify both endogenous and truncated *ERECTA* revealed that the amounts of *ΔKinase* transcripts were at levels comparable to those of the endogenous *ERECTA* transcripts (Figure 2A). Therefore, the increased amount of ΔKinase

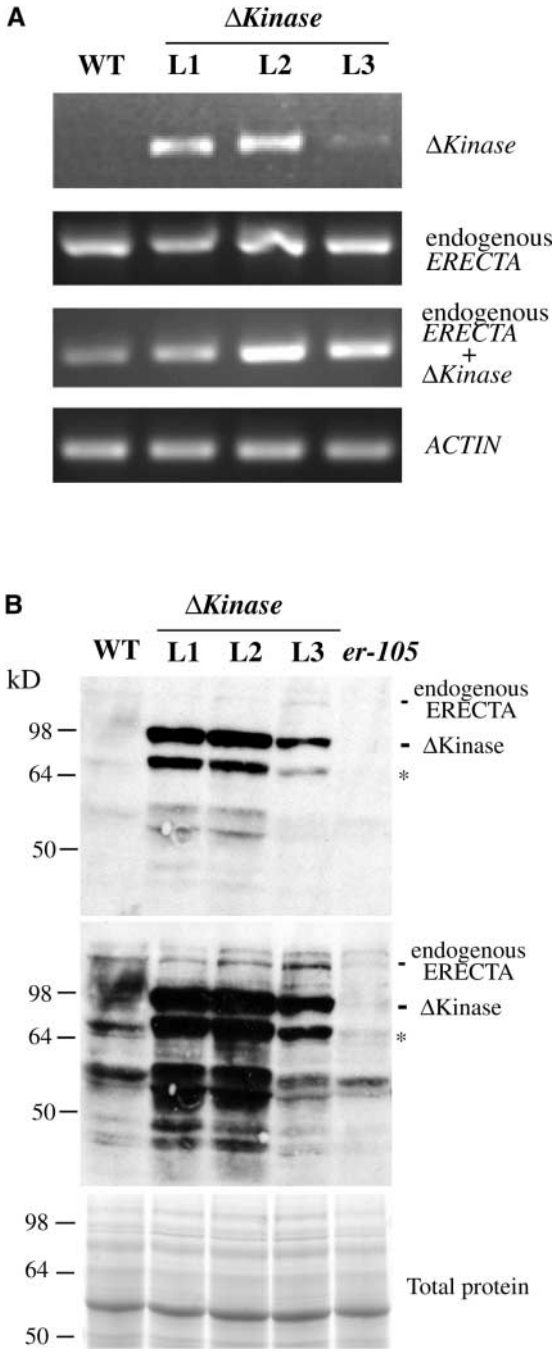

Figure 2. Dominant-Negative Effects in *ΔKinase* Are Caused by the Presence of the Truncated Receptor and Not by the Cosuppression of Endogenous *ERECTA*.

(A) Semiquantitative RT-PCR analysis of the *ΔKinase* and *ERECTA* transcripts in buds and flower clusters of the wild type (WT) and three independent *ERECTA*::*ΔKinase* lines (L1, L2, and L3). The top gel shows that expression levels of *ΔKinase* correlate with the severity of the phenotype. The second gel shows the lack of cosuppression revealed by primers that specifically amplify the endogenous *ERECTA* transcripts. In the third gel, primers that amplify both endogenous *ERECTA* and the *ΔKinase* transcripts revealed that *ΔKinase* transcripts are present at a level comparable to that in the endogenous *ERECTA*. The bottom gel represents an actin fragment amplified simultaneously as a control.

(B) Immunoblot analysis of protein extracts from buds and flower clusters of the wild type, three independent *ERECTA*::*ΔKinase* lines, and the null allele *erecta-105*. In the top gel, a blot exposed for a short period (3 to 5 min) shows that the amount of the ΔKinase protein correlates with the amount of its message. The identical blot in the middle was exposed for a longer period (~50 min) to detect the endogenous ERECTA protein, which was present at much lower levels compared with ΔKinase. At bottom, a Coomassie blue–stained gel shows the total proteins. Asterisks indicate cleaved ΔKinase protein. Numbers at left indicate molecular mass markers in kilodaltons.

was associated with post-transcriptional regulation, most likely as a result of the increased stability of the truncated protein. From these results, we conclude that the observed erecta phenotype of *ERECTA*::*ΔKinase* transgenic plants most likely is conferred by dominant-negative interference of highly stable ΔKinase protein with the endogenous ERECTA pathway.

Both RT-PCR with primers specific to the *ΔKinase* transgene and immunoblot analysis demonstrated that *ERECTA*::*ΔKinase* was expressed at a level three times greater in the lines with severe phenotype (L1 and L2) than in the line with mild phenotype (L3) (Figures 2A and 2B). Thus, the phenotypic severity correlates with the amount of *ΔKinase* gene products in a dosage-dependent manner.

A ΔKinase Fragment Further Enhances the Growth Defects in the Null Allele of *erecta*

The dominant-negative effects of ΔKinase were quite surprising, given that similar deletion mutants in CLV1 and Xa21 (e.g., *clv1-6* and *Xa21-D*) have been shown to retain partial function (Clark et al., 1997; Wang et al., 1998; Torii, 2000). Therefore, we sought to determine the underlying mechanism of the dominant-negative interference. If the ERECTA signaling pathway is strictly homodimeric and linear, we predict that the expression of ΔKinase will not enhance the erecta null phenotype. By contrast, ΔKinase may make the erecta null phenotype even more severe if the ERECTA signaling pathway is redundant. To address these hypotheses, we introduced *ERECTA*::*ΔKinase* into *erecta-105* plants, which do not produce any *ERECTA* transcripts (Torii et al., 1996; Lease et al., 2001b). Expression of *ΔKinase* in *erecta-105* conferred severe growth defects (Figures 3 and 4). The transgenic plants were dwarf, with extremely short internodes, pedicels, and siliques as well as smaller, round flowers (Figures 3A to 3C). The development of flower organs seemed less coordinated, and pistils protruded above buds (Figure 3B).

ERECTA::*ΔKinase–c-Myc*, which contains a triple c-Myc sequence (EQKLISEEDL) at the end, retained the ability to exaggerate the erecta null phenotype, albeit slightly less effectively (Figures 3A to 3D). This finding could be attributable to steric hindrance by the triple c-Myc peptides or, alternatively, to reduced accumulation of the gene products (Figure 4B). Immunoblot analysis revealed that ΔKinase–c-Myc was detected by both anti-ERLRR and anti-c-Myc antibodies as a band of ~105

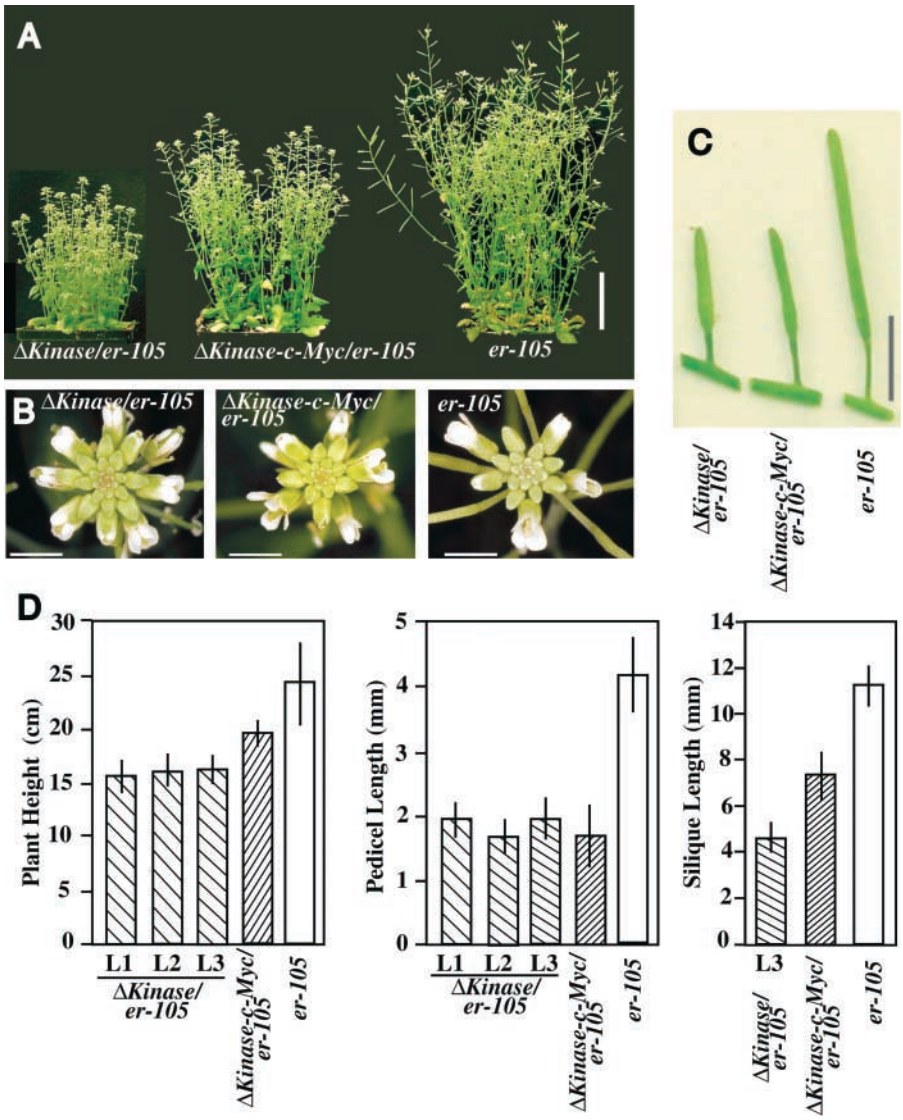

Figure 3. Expression of *ΔKinase* Enhances the Growth Defects in the Null *erecta* Allele.

(A) Seven-week-old plants of *erecta-105*, *ΔKinase/erecta-105*, and *ΔKinase–c-Myc/erecta-105*. Bar = 4 cm.
(B) Inflorescence apices from *erecta-105*, *ΔKinase/erecta-105*, and *ΔKinase–c-Myc/erecta-105*. Bars = 3 mm.
(C) Siliques and attached pedicels of *erecta-105*, *ΔKinase/erecta-105*, and *ΔKinase–c-Myc/erecta-105*. Bar = 5 mm.
(D) Morphometric analysis of fully grown 7-week-old plants of *erecta-105*, three independent transgenic lines of *ERECTA*::*ΔKinase/erecta-105* (L1, L2, and L3), and one line of *ERECTA*::*ΔKinase–c-Myc/erecta-105*. Plant (inflorescence) height, pedicel length, and silique length were measured as described for Figure 1E. The length of the siliques was measured in only one line of *ERECTA*::*ΔKinase/erecta-105* (L3), because the other two lines had reduced fertility as a result of short filaments. Bars represent average values ± SD.

kD, slightly larger than the nontagged ΔKinase (Figure 4B). The anti-c-Myc antibody was highly specific and essentially gave no background signal (Figure 4B).

Although both ΔKinase and ΔKinase–c-Myc confer phenotypes much more severe than that of *erecta-105* or any of the available 24 *erecta* alleles (Lease et al., 2001a), the phenotypic characteristics, such as compact inflorescence and short, blunt siliques, were consistent with the *erecta* defects (Figure 3). Together, these data support our hypothesis that nonfunctional ΔKinase is capable of interfering with and shutting down the ERECTA and related RLK pathways that regulate organ elongation in a partially redundant manner (see Discussion).

The Highly Accumulated ERECTA ΔKinase Fragment Does Not Interfere with the CLV1 LRR-RLK Signaling Pathway

Use of the endogenous *ERECTA* promoter and terminator should minimize the ectopic effects of ΔKinase. However, it is possible that a highly stable ΔKinase fragment associates in a nonspecific manner with RLKs that are expressed in the same tissue/cell

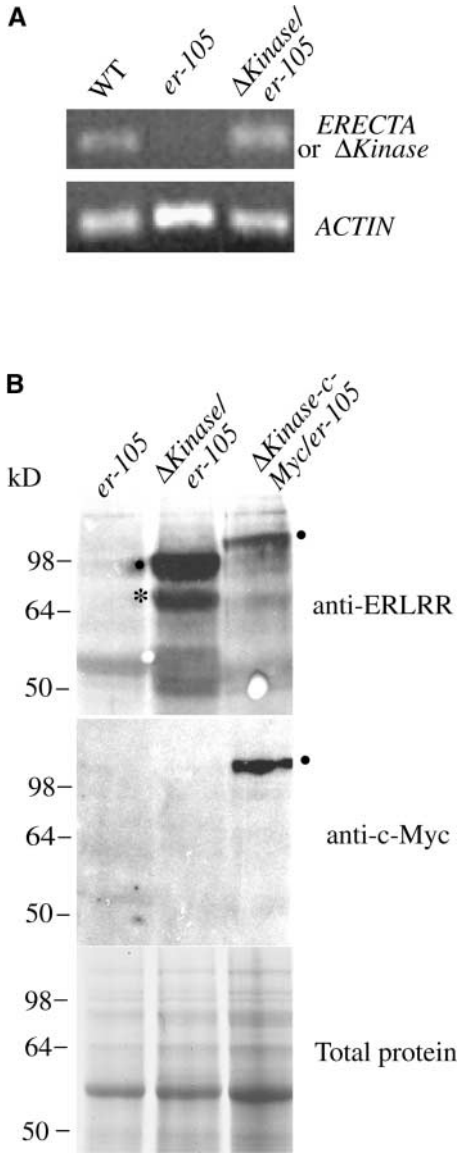

Figure 4. Accumulation of *ΔKinase* Transcripts and ΔKinase and ΔKinase–c-Myc Proteins in Transgenic *erecta-105* Plants.

(A) Semiquantitative RT-PCR analysis of *ERECTA* and *ΔKinase* transcripts from buds and flower clusters of wild-type (WT), *erecta-105*, and *ERECTA*::*ΔKinase*/*erecta-105* plants. *ΔKinase* transcripts are expressed in the transgenic *erecta-105* plants at a level similar to that of the endogenous *ERECTA* transcripts in wild-type plants. The *erecta-105* plants do not express any *ERECTA* transcripts. Primers annealing to the LRR-coding region of *ERECTA* were used for PCR. An actin fragment was amplified simultaneously as a control.

(B) Protein immunoblot analysis. At top, a blot probed with anti-ERLRR antibodies shows the accumulation of the ΔKinase and ΔKinase–c-Myc proteins in transgenic *erecta-105* plants. The identical blot in the middle was probed with anti-c-Myc antibodies and shows the accumulation of the ΔKinase–c-Myc protein. At bottom, a Coomassie blue–stained gel shows the total proteins. Numbers at left indicate molecular mass markers in kilodaltons. Dots indicate the transgene products. An asterisk indicates cleaved ΔKinase protein.

types as *ERECTA* but that do not normally interact with the ERECTA signaling pathway. We sought to determine whether the dominant-negative ΔKinase inhibits a well-studied RLK signaling pathway that has overlapping expression patterns with ERECTA.

For this purpose, we investigated whether *ERECTA*::*ΔKinase* inhibits the CLV1 signaling pathway. *CLV1* is expressed at the subepidermal layers in the center of the shoot and flower meristems, whereas *ERECTA* is expressed broadly within these meristems (Clark et al., 1997; Yokoyama et al., 1998); therefore, ΔKinase likely accumulates in the cells in which CLV1 normally functions. The hallmark of the clv phenotype is an increased number of floral organs as a result of enlarged floral meristems (Leyser and Furner, 1992; Clark et al., 1993). Although the wild-type flower has two carpels, average carpel numbers of the severe allele *clv1-4* and the weak allele *clv1-6* are 5.12 $\pm$ 0.04 and 3.91 $\pm$ 0.04, respectively (Yu et al., 2000). As shown in Figure 5A, carpel numbers were not affected by the expression of *ERECTA*::*ΔKinase*. Wild type, *erecta-105*, *ΔKinase* in wild-type, and *ΔKinase* in *erecta-105* all produced siliques with two carpels (2.00 $\pm$ 0.00, $n = 40$ for each genotype).

Molecular-genetic studies have shown that the CLV signaling pathway restricts the expression domain of *WUSCHEL* (*WUS*), which specifies stem cell fate (Brand et al., 2000; Schoof et al., 2000). Unlike *clv* mutations, which confer ectopic upregulation of *WUS* expression (Brand et al., 2000; Schoof et al., 2000), our semiquantitative RT-PCR analysis revealed that *ERECTA*::*ΔKinase* had no effect on *WUS* expression levels (Figure 5B). From these phenotypic and molecular analyses, we conclude that highly accumulated ΔKinase does not interfere with the CLV signaling pathway.

These findings suggest that the components of ERECTA and CLV signaling pathways are quite distinct, even though the structural features of these two LRR-RLKs are similar. Therefore, we investigated whether ERECTA associates with a known component of the CLV pathway, Kinase-Associated Protein Phosphatase (KAPP). KAPP associates with the kinase domains of several RLKs, including RLK5/HAESA and CLV1, via its kinase interaction domain (KID) (Stone et al., 1994, 1998; Williams et al., 1997). We expressed both wild-type and kinase-inactive forms of ERECTA fused to the maltose binding protein. The kinase-inactive version (K676E) has a substitution of an invariant Lys in subdomain II to Glu. The interaction of ERECTA with the KAPP KID was tested by dot-blot analysis, because it gave stronger signals than electroblotted samples. As shown in Figure 5C, positive signal was detected only in the kinase-active form of RLK5/HAESA, which was used as a positive control. Because ERECTA possesses Ser/Thr protein kinase activity (Lease et al., 2001a), we conclude that ERECTA does not associate with KAPP in vitro. These results indicate that the expression of the ΔKinase fragment of ERECTA does not affect the CLV1 pathway, which most likely operates in a distinct manner; they further imply that the dominant-negative effects of ΔKinase involve specific mechanisms.

A Functional LRR Domain of ERECTA Is Required for the Dominant-Negative Effects

To gain more insight into the mechanisms of ΔKinase action, we introduced into the ΔKinase fragment a point mutation cor-

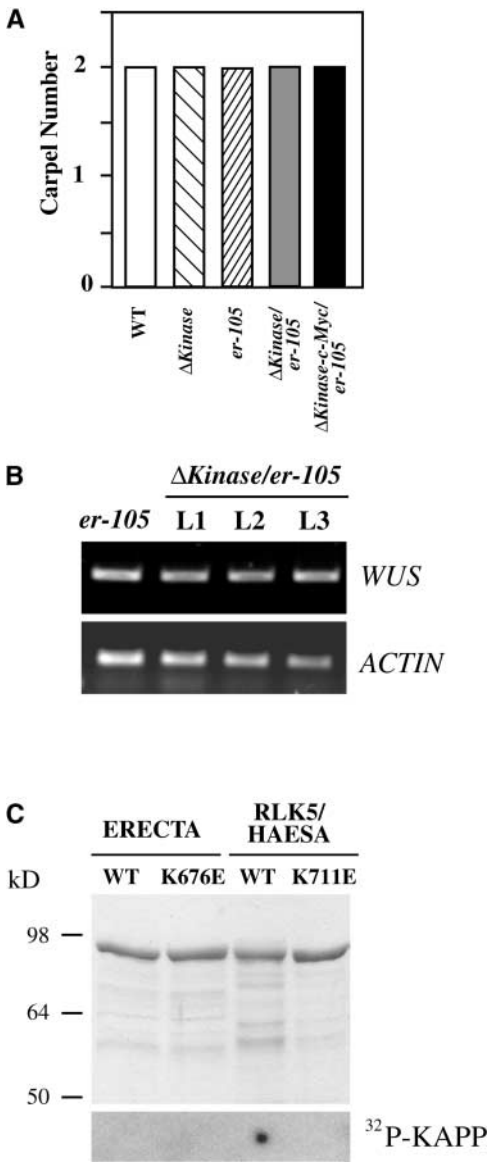

Figure 5. Expression of ΔKinase Does Not Interfere with the CLV Signaling Pathway, and ERECTA Does Not Associate with KAPP, a Negative Regulator of Multiple RLKs, Including CLV1.

(A) Number of carpels in wild-type (WT), *ercta-105*, *ERECTA*::*ΔKinase*/ wild type (L1), *ERECTA*::*ΔKinase*/*ercta-105* (L3), and *ERECTA*::*ΔKinase–c-Myc*/*ercta-105* flowers. Bars represent mean values ($n = 40$) for each genotype.

(B) Semiquantitative RT-PCR analysis of *WUS* transcripts from buds and flower clusters of *ercta-105* and three independent lines of *ERECTA*::*ΔKinase*/*ercta-105* plants. *WUS* expression levels are unaltered by the ΔKinase fragment.

(C) KAPP KID does not associate with an active kinase catalytic domain of ERECTA. Top, Coomassie blue–stained SDS-PAGE gel of the affinity-purified, recombinant ERECTA and RLK5/HAESA kinase domains, both active (WT) and inactive (for ERECTA, K676E; for RLK5, K711E) forms, fused to the maltose binding protein. One microgram of the purified proteins was loaded on the gel. Molecular mass markers are indicated at left. Bottom, Autoradiogram of the purified proteins dot-blotted onto a polyvinylidene difluoride membrane and probed with the ^{32}P-labeled GST-KID fusion protein.

responding to *ercta-103*, which replaces the Met within the 10th LRR with Ile (M282I) (Torii et al., 1996) (Figure 6A). Introduction of the mutation did not result in reduced stability of the transcripts or proteins; instead, the amount of the $\Delta Kinase_{M282I}$ protein appeared to have increased slightly (Figure 6B). Nevertheless, the M282I mutation severely compromised the dominant-negative effects of ΔKinase, because transgenic *ercta-105* plants expressing $\Delta Kinase_{M282I}$ no longer displayed severe dwarfism, extreme compact inflorescence, or reduced fertility (Figure 6C). These results indicate that a functional LRR domain is required for the dominant-negative interference and imply that structural integrity of the extracellular LRR domain may be crucial for titrating ligand or receptor partners that are shared by RLKs, which possess overlapping function with ERECTA.

Dominant-Negative ΔKinase Migrates as a Protein Complex in the Absence of Endogenous ERECTA

If ΔKinase confers dominant-negative interference through direct association with the components (such as ligands and partners) of related RLKs, we would expect ΔKinase to form a protein complex. To test this hypothesis, we investigated the behavior of ΔKinase by gel-filtration chromatography. Flowers and bud clusters of transgenic *ercta-105* plants expressing either ΔKinase or ΔKinase–c-Myc were used as materials to minimize the complications of having both full-length and truncated ERECTA. In the presence of 1% Triton X-100, the ΔKinase protein migrated as a complex of ~400 kD (Figure 7, top gel). No signal of similar size was detected in the control *ercta-105* fractions (Figure 7, middle gel). Some ΔKinase may exist at ~100 kD, representing monomers. The presence of nonspecific signals of similar size in the control *ercta-105* fractions, however, makes this possibility inconclusive (Figure 7). The immunoblot probed with anti-c-Myc antibodies revealed that ΔKinase–c-Myc migrated exclusively as a complex of a similar size with a slightly broader range of elution, which may be the result of less efficient interactions of ΔKinase–c-Myc with other components caused by steric hindrance (Figure 7, bottom gel). The fact that ΔKinase migrated as a protein complex in the absence of the endogenous ERECTA is consistent with our hypothesis that the physical interaction of nonfunctional ΔKinase with the other RLKs enhances the organ elongation defects in *ercta-105*.

ERECTA Regulates Proper Cell Proliferation and Polarity

To understand how ERECTA controls organ elongation, we analyzed the cellular defects in *ercta* and in dominant-negative transgenic plants. Mature pedicels were examined, because

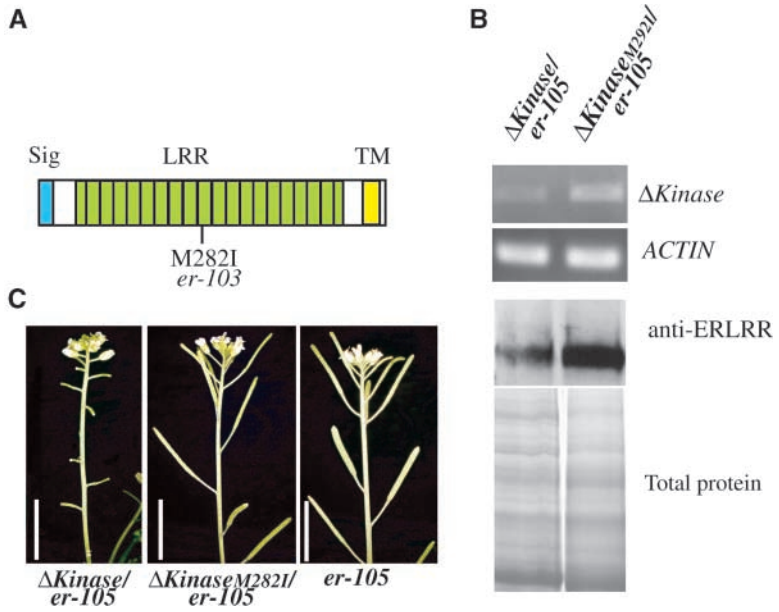

Figure 6. A Functional LRR Domain of ΔKinase Is Required for the Dominant-Negative Interference.

(A) Scheme showing the location of an introduced point mutation corresponding to *erecta-103*, which replaces the Met at amino acid 282 with Ile. TM, transmembrane domain; Sig, signal peptide.

(B) The M282I mutation in ΔKinase does not lead to reduced transcript and protein levels. The top two gels show semiquantitative RT-PCR analysis of *ΔKinase* and control actin transcripts in buds and flower clusters of *ERECTA*::*ΔKinase/erecta-105* (L1) and *ERECTA*::$\Delta Kinase_{M282I}$ */erecta-105* plants. The third gel shows protein immunoblot analysis of extracts from buds and flower clusters of *ERECTA*::*ΔKinase/erecta-105* (L1) and *ERECTA*::$\Delta Kinase_{M282I}$ */erecta-105* plants probed with anti-ERLRR antibody. The Coomassie blue–stained gel at bottom shows the total proteins.

(C) The M282I mutation in ΔKinase severely compromises the dominant-negative effects. Shown are side views of the main inflorescences of *ERECTA*::*ΔKinase/erecta-105* (L1), *ERECTA*::$\Delta Kinase_{M282I}$ */erecta-105*, and *erecta-105* plants. Bars = 1 cm.

the degree of allelic severity correlates with reduction in pedicel length (Torii et al., 1996; Lease et al., 2001a). Figure 8 shows representative, longitudinal sections of fully expanded mature pedicels. Although the wild-type pedicels were approximately twice as long as *erecta-105* pedicels (Figure 1D), cells in the cortex and endodermis of *erecta-105* were notably larger than wild-type cells, indicating that the short pedicel phenotype is attributable to fewer cells (Figures 8A and 8C). Moreover, cortex cells were expanded radially, accounting for the thick pedicel phenotype of *erecta* (Figure 8C). The epidermal cells of *erecta-105* were slightly shorter than the wild-type cells. We detected no significant difference in the pith (data not shown). Our observations indicate that *erecta* is not a typical dwarf mutant with general cell elongation defects.

Similar to the *erecta* mutation, the ΔKinase protein conferred reduced cell numbers associated with enlarged and irregular cell shape in the cortex and endodermis (Figure 8). However, unlike *erecta-105*, ΔKinase cortex cells were not expanded laterally. In the *ERECTA*::*ΔKinase/erecta-105* pedicels, disorganized cell growth in the cortex was even more evident (Figure 8D). Although some cells in the cortex were large and expanded, others remained small, leaving many "gaps" between the cells. These observations suggest that *ERECTA* and its overlapping pathways are required for coordinated cell proliferation and proper cell–cell interactions within the cortex cell layers.

Increased Levels of Somatic Endoploidy in Pedicels of *erecta* and ΔKinase Plants

Increased cell size in general correlates with increased DNA content or ploidy level (Kondorosi et al., 2000). Because mature pedicels of *erecta* and *ΔKinase* have enlarged cortex cells, we measured their ploidy levels to determine whether the inhibition of ERECTA signaling leads to somatic endoploidy. A majority (62%) of nuclei in the wild-type pedicels remained diploid (2C), whereas some were tetraploid (4C; 31%) and a few were octaploid (8C; 7%) (Figure 8E). Both intermediate allele *erecta-103* and *ΔKinase* pedicels showed increases in the 4C nuclei (37 and 36%, respectively), making the 2C/4C ratio 1.5, in contrast to 2.0 in the wild-type pedicels (Figures 8E and 8F). The 4C nuclei content was highest in the null allele *erecta-105* pedicels (49%; 2C/4C ratio = 0.9), whose cortex cells were the largest (Figure 8). Therefore, the degree of *erecta* defects and cortex cell size have a positive correlation with increased 4C content. The expression of *ΔKinase* in *erecta-105* did not confer an additional increase in 4C content (47%; 2C/4C ratio = 0.97) (Figures 8E and 8F). This finding is consistent with our histological observation that *ΔKinase/erecta-105* did not lead to extra cell enlargement but rather disrupted the proper coordination of cortex cell development (Figure 8D). None of the genotypes showed increased amounts of 8C (Figure 8E), indicating that in-

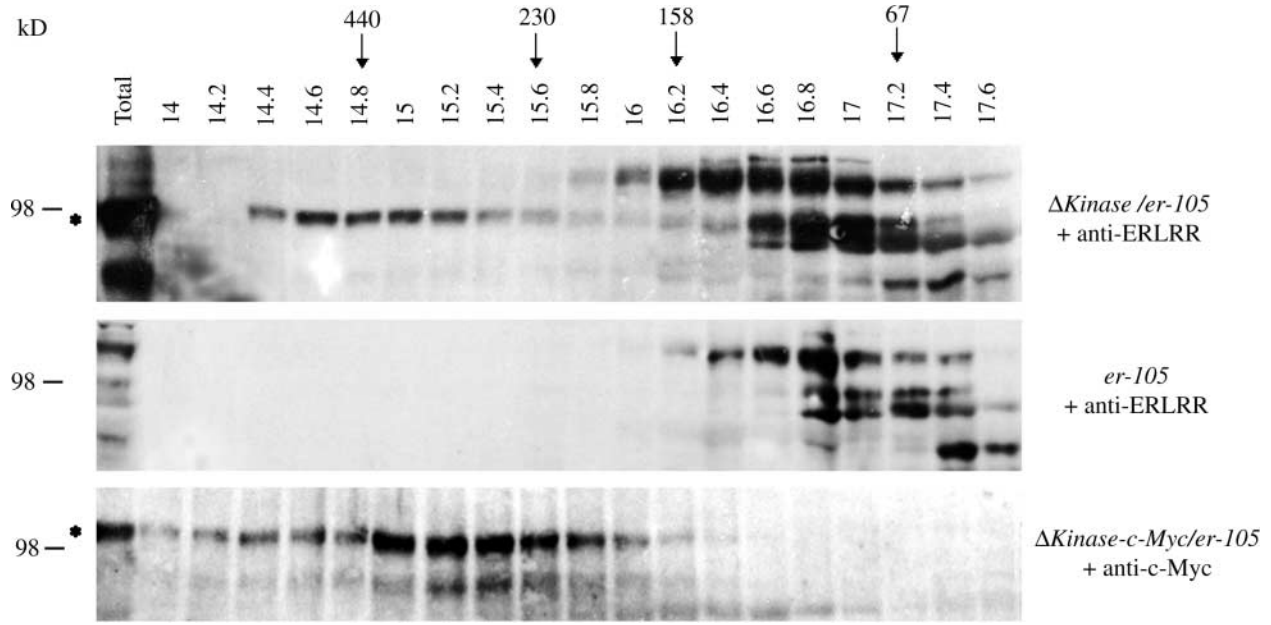

Figure 7. Both ΔKinase and ΔKinase–c-Myc Proteins Migrate as an ~400-kD Protein Complex in the Absence of the Endogenous ERECTA Protein.

Total proteins (for ΔKinase) or membrane proteins (for ΔKinase–c-Myc) isolated from buds and flower clusters were separated by gel-filtration chromatography (see Methods). Each fraction was separated by SDS-PAGE. Total proteins were loaded in the first lane for comparison. Numbers above each lane refer to the elution volume (in milliliters) of the corresponding fraction. The elution peaks of molecular mass standards for gel-filtration chromatography are indicated at top (arrows). Molecular mass standards for SDS-PAGE are indicated at left. The top gel shows the detection of the ΔKinase complex (asterisk) in transgenic *ERECTA*::*ΔKinase/ecta-105* plants on an immunoblot probed with anti-ERLRR antibodies. The middle gel shows a control immunoblot of *ecta-105* fractions probed with anti-ERLRR antibodies. The bottom gel shows the detection of the ΔKinase–c-Myc complex (asterisk) in transgenic *ERECTA*::*ΔKinase–c-Myc/ecta-105* plants on an immunoblot probed with anti-c-Myc antibodies.

hibition of the ERECTA pathway does not activate endoreduplication cycles. Because mature pedicels do not express the cell-cycling marker *Cyc1At*::*GUS* (K.U. Torii, unpublished data), it is very unlikely that the 4C nuclei represent actively proliferating S-phase cells. Together, our findings suggest that *erecta* mutations and *ΔKinase* expression may inhibit cell division and promote premature differentiation of the 4C cells.

DISCUSSION

In this study, we provide evidence that truncated ERECTA lacking the cytoplasmic kinase domain (ΔKinase) confers dominant-negative effects in Arabidopsis organ growth and internodal elongation. Biochemical and phenotypic analyses of the null *erecta* allele expressing ΔKinase revealed the presence of multiple interrelated pathways that act together with ERECTA to coordinate cell proliferation and cell expansion within the same cell types.

Modes of Action of ERECTA and Redundancy in the ERECTA Signaling Pathway Revealed by ΔKinase Expression

Unlike animal receptor kinases, the kinase domains of some plant LRR-RLKs appear partially dispensable. For instance, two *clv1* alleles that truncate the entire kinase domain, *clv1-6* and *clv1-7*, have the weakest phenotypes (Clark et al., 1997). Expression of Xa21D, a naturally occurring variant of the rice disease resistance gene that lacks the entire kinase domain, confers partial resistance to a full spectrum of pathogens (Wang et al., 1998). A model for Xa21D action is that it forms a functional heterodimer with an RLK, which lacks ligand recognition specificity, and that ligand binding to the LRR domain of Xa21D stimulates the phosphorylation of its receptor partner and initiates signaling (Wang et al., 1998). By contrast, expression of the ΔKinase form of ERECTA resulted in an inhibition of normal ERECTA functions (Figures 1 and 2). Based on the analogy from animal receptor kinase signaling, it is reasonable to hypothesize that ΔKinase forms a nonfunctional receptor dimer with the endogenous receptor partner of ERECTA and prevents the transphosphorylation that is a prerequisite for the activation of the signaling cascades.

In the absence of endogenous ERECTA protein, ΔKinase migrates as an ~400-kD protein complex, which most likely represents a nonfunctional receptor oligomer (Figure 5), suggesting that ERECTA may function as a heterooligomer. Some plant LRR-RLKs function as heterodimers. For example, CLV1 forms a heterodimer CLV2 LRR transmembrane protein, presumably via disulfide linkage (Jeong et al., 1999; Trotochaud et al., 1999). Recently, the Arabidopsis BAK1 LRR-RLK was identified as a receptor partner of BRI1 in BR signaling (Li et al., 2002; Nam and Li, 2002).

The apparent discrepancy in the recessive nature of *erecta*

mutations and the dominant effects of *ERECTA*::*ΔKinase* can be explained by the high level of accumulation of ΔKinase protein. Although the mRNA levels of *ΔKinase* and endogenous *ERECTA* are similar, the amount of the ΔKinase protein is ~100-fold greater than that of the full-length ERECTA protein, most likely as a result of increased protein stability (Figures 2 and 4). In animals, ligand-induced degradation of the epidermal growth factor RTK plays an important role in the downregulation of epidermal growth factor signaling (Beguinot et al., 1984; Jones et al., 2002). Similarly, the amount of endogenous ERECTA RLK may be regulated tightly during organogenesis. Perhaps the truncated ΔKinase is not under such regulation; thus, it stably locks in and sequesters the signaling components.

Although highly accumulated ΔKinase protein also may interfere with factors that normally do not interact with the endogenous ERECTA, we believe that the observed dominant-negative interference is highly specific for the following reasons. First, the growth defects conferred by ΔKinase resemble or exaggerate the phenotypes of the *erecta* mutations, both in overall plant morphology and in underlying cellular defects (Figures 1, 3, and 8). Second, the *ERECTA cis* regulatory sequences that we used to express *ΔKinase* contain information sufficient for the proper expression of *ERECTA*, because a full-length *ERECTA* clone with these regulatory sequences fully complements *erecta* mutants (K.U. Torii, unpublished data). Therefore, neomorphic effects of ΔKinase in different tissue/cell types should be minimized. Third, ΔKinase did not inhibit the CLV LRR-RLK signaling pathway, which operates in the same cells that express ERECTA within the shoot and flower meristems (Figure 5). Fourth, introduction of a point mutation in the LRR

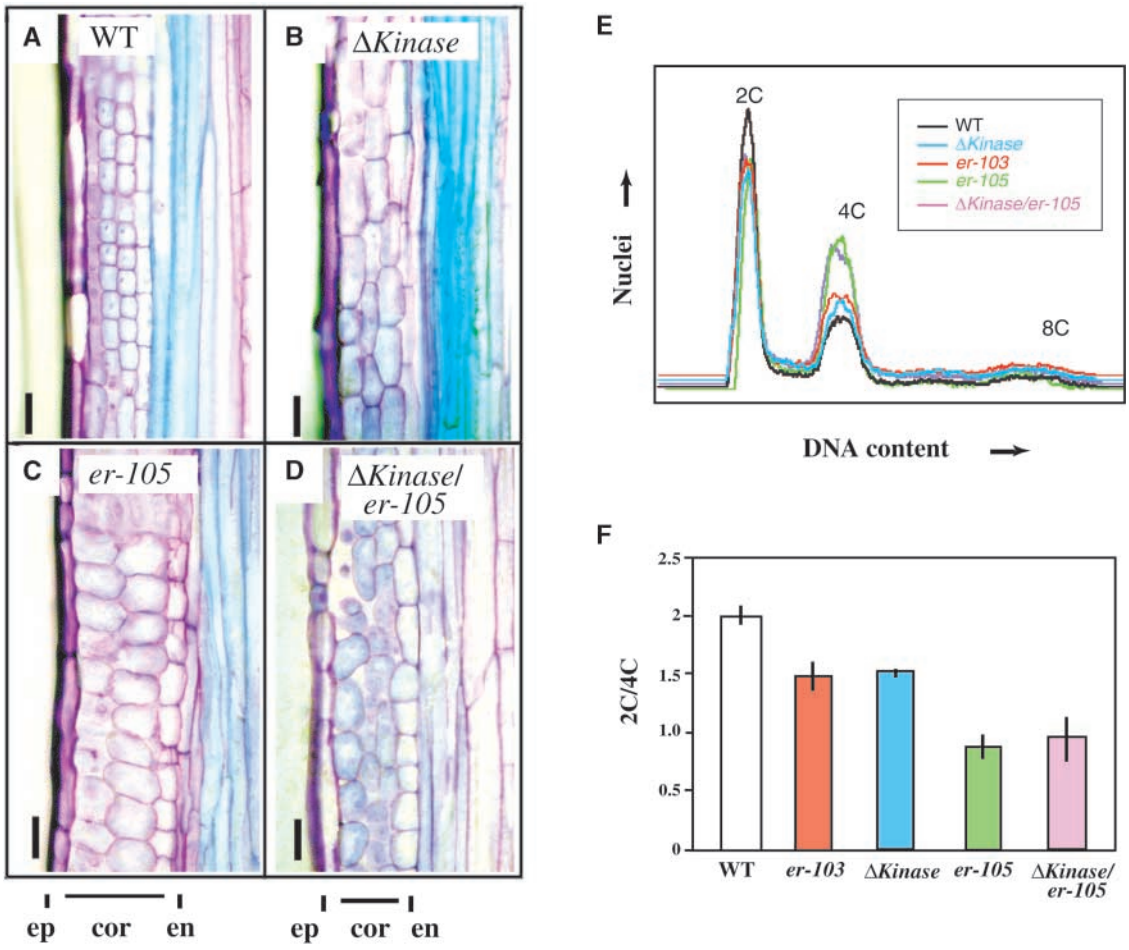

Figure 8. *erecta* Mutation and ΔKinase Expression Lead to Aberrant Cell Enlargement, Reduced Cell Numbers in the Cortex, and Increased Endoploidy in Mature Pedicels.

(A) to **(D)** Longitudinal sections of mature pedicels from wild-type (WT) **(A)**, *ERECTA*::*ΔKinase* **(B)**, *erecta-105* **(C)**, and *ERECTA*::*ΔKinase/erecta-105* **(D)** plants. Photographs were taken at the same magnification. cor, cortex; en, endodermis; ep, epidermis. Bars = 25 μm.

(E) and **(F)** Flow cytometric analysis of mature pedicels from wild-type, intermediate allele *erecta-103*, *ERECTA*::*ΔKinase*, null allele *erecta-105*, and *ERECTA*::*ΔKinase/erecta-105* plants. **(E)** shows representative nuclei counts, and **(F)** shows the 2C/4C ratio as an average of four independent counts. Error bars indicate standard errors.

domain of ΔKinase abolished the dominant negative effects without affecting the stability of the transcripts/proteins (Figure 6). This finding suggests that proper interaction with ligands and/or receptor partners that normally associate with native ERECTA likely are required for the observed dominant-negative interference, rather than the ~100-fold accumulation of the protein causing some cellular toxicity.

The notion that having truncated ERECTA protein is worse than having none at all for Arabidopsis organ and internodal growth suggests complex redundancy in the signaling pathways involving ERECTA. One possible model is that several RLKs are capable of perceiving the same signal as ERECTA and of regulating partially overlapping pathways (Figure 9). ΔKinase may take up and deplete ligands and/or receptor partners of ERECTA that are shared by other RLKs and thus shut down whole pathways, which could operate in either a parallel or a convergent manner (Figure 9). The fact that a functional LRR domain is required for dominant-negative interference supports this hypothesis (Figure 6).

Such intricacy in signal transduction is well known in numerous animal receptor kinases. For example, mammalian platelet-derived growth factor (PDGF) exists as a homodimer and as heterodimers of three homologous polypeptides: PDGF A, B, and C (such as AA, AB, and BB) (Ataliotis and Mercola, 1997; Li et al., 2000). Two PDGF RTKs, PDGFαR and PDGFβR, recognize different PDGF isoforms with distinct affinity (Ataliotis and Mercola, 1997). This complex ligand receptor recognition property provides overlapping yet unique functions for PDGF signaling during mammalian embryogenesis. Consistently, expression of the dominant-negative ΔKinase form of PDGFR suppressed diverse signal transduction pathways mediated by multiple PDGF isoforms (Ueno et al., 1993). Similar complexity is documented for fibroblast growth factor RTK signaling pathways (Givol and Yayon, 1992).

The formation of an ~400-kD ΔKinase protein complex is consistent with recent reports that plant LRR receptors constitute membrane-associated complexes (Trotochaud et al., 1999; Rivas et al., 2002a, 2002b). However, the components of the receptor complex could be distinct among CLV1, Cfs, and ERECTA. For instance, although active CLV1 complex contains KAPP and ROP small GTPase, neither is in the Cf4 or Cf9 complex (Trotochaud et al., 1999; Rivas et al., 2002a, 2002b). We found that ERECTA does not associate with KAPP (Figure 5C). Because the ΔKinase complex is nonfunctional, it also is unlikely to contain cytoplasmic factors that are recruited to the complex in a phosphorylation-dependent manner, such as ROP (Trotochaud et al., 1999). On the other hand, by analogy to the animal dominant-negative receptor kinases, the ΔKinase complex likely contains ligands and receptor partners for ERECTA and related RLKs (Figure 9). This notion is consistent with our finding that the point mutation within the LRR domain disrupts dominant-negative interference (Figure 6).

No matter how carefully our experiments were designed, we could not completely eliminate the possibility of nonspecific, neomorphic effects by ΔKinase. For instance, ~100-fold accumulation of ΔKinase could titrate ligands for RLKs that have functions distinct from those of ERECTA, even if these ligands possess lower, and biologically irrelevant, affinity to the LRR

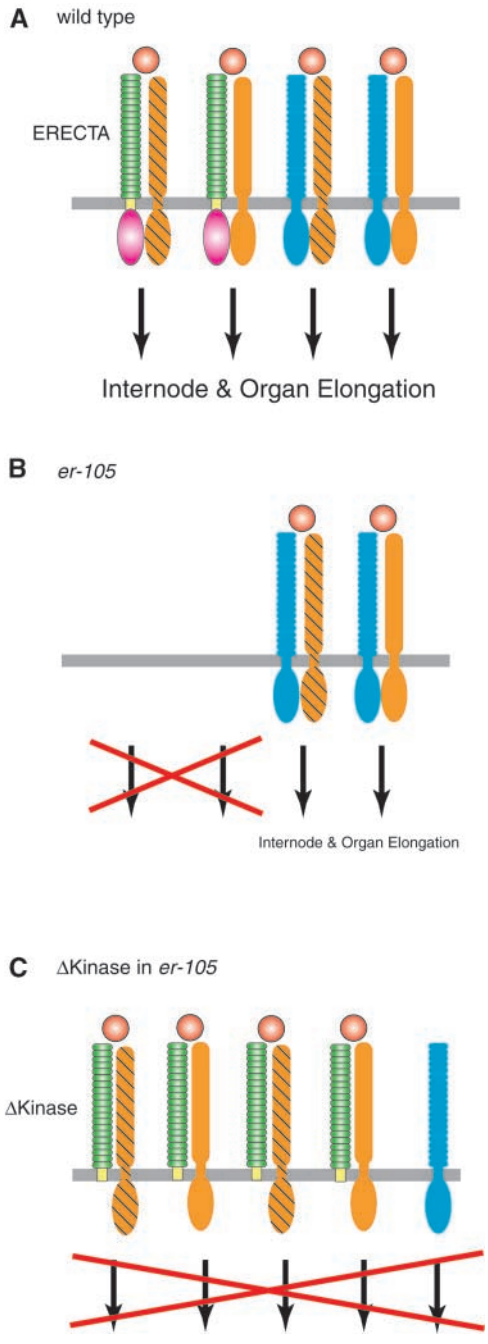

Figure 9. Hypothetical Model for the ERECTA Signaling Pathway and ΔKinase Action.

(A) In wild-type plants, ERECTA associates with multiple partners (orange). Additional RLKs (blue) may share ligands (red) as well as receptor partners of ERECTA. The activation of these pathways promotes internode/organ elongation.

(B) *erecta-105* plants do not have any ERECT. However, the receptor complex with overlapping function partially promotes internode/organ elongation.

(C) In *ERECTA*::*ΔKinase*/*erecta-105* plants, highly stable ERECTA ΔKinase fragments shut down the entire pathway, presumably by forming inactive receptor heterodimers and/or depleting ligands for the RLK that has a function partially redundant with that of ERECTA.

domain of ERECTA. Another possibility is that the presence of ΔKinase alters the cellular equilibrium of cytoplasmic proteins involved in the regulation of multiple RLKs with distinct, unrelated functions. The availability of such proteins may decrease if, in wild-type plants, they interact with the ERECTA complex and then are recycled. KAPP is known to associate with a range of LRR-RLKs (Braun et al., 1997). Although we have shown that KAPP does not interact with ERECTA (Figure 5C), it might interact with a hypothetical ERECTA partner. Other unidentified downstream components of multiple RLKs also might be affected by ΔKinase. In any event, purification of the highly stable ΔKinase complex and subsequent isolation of the components of the ERECTA signaling pathway, as well as identification of the RLKs that possess redundant functions with ERECTA, will provide a complete picture of the biochemical mechanism of dominant-negative interference.

Role for the ERECTA Signaling Pathway in Organ Growth

Our observations revealed that *erecta* confers greatly increased cell size, primarily in the cortex, despite the fact that overall organ elongation is inhibited strongly (Figures 1 and 6). This finding is in contrast to what is known about almost all dwarf mutants described to date, which have reduced cell size, including those defective in biosynthesis and/or the perception of hormones such as auxins, gibberellins, and BRs (Timpte et al., 1992; Szekeres et al., 1996; Azpiroz et al., 1998; Fridborg et al., 1999), and indicates that *ERECTA* does not promote the general cell elongation process. The cellular defects in *erecta* are rather similar to the inhibition of cell cycle progression, which leads to cell enlargement even though overall plant size is reduced (Wang et al., 2000; De Veylder et al., 2001). One possible explanation for these findings is that *ERECTA* is required for proper cell cycle progression. Consistent with this hypothesis, the ratio of 4C cells increased in both *erecta* and *ΔKinase* plants (Figures 8E and 8F). Perhaps in the absence of the ERECTA signal, the cortex cells in pedicels may not enter mitosis and instead undergo premature differentiation at the G2 stage. Detailed analysis of cell division patterns during pedicel development is required to test this hypothesis. In contrast to the findings in *erecta*, overexpression of the cyclin kinase inhibitors (ICKs/KRPs) in Arabidopsis reduced the ratio of 4C cells in the leaf as a result of slowed cell cycle progression and reduced endoreduplication (De Veylder et al., 2001). Therefore, ERECTA signaling and ICKs/KRPs may act on distinct aspects of cell proliferation.

The striking cellular phenotype of the *ΔKinase/erecta-105* pedicels is the loss of organized cortex cell size and shape (Figure 8D), suggesting that a loss of the entire pathway not only inhibits cell proliferation but also disrupts the uniformity of cell proliferation. Perhaps ERECTA and overlapping signaling pathways provide positional cues for coordinated proliferation among cells of the same type and such coordination is essential for proper organ elongation. Identification of the ligands and receptor partners of ERECTA, and analysis of their tissue- and/or cell-specific localization, will reveal the source of the signals and their target cells and will provide a clear picture of ERECTA LRR-RLK signaling in organogenesis.

ΔKinase as a Potential Tool to Dissect RLK Signal Transduction in Plants

The dominant-negative approach using truncated receptor kinases has been instrumental in dissecting signal transduction pathways and elucidating the in vivo functions of animal receptor kinases. For example, microinjection of the ΔKinase forms of the fibroblast growth factor RTK and the activin (transforming growth factor β) receptor Ser/Thr kinase revealed their essential roles in mesoderm formation during *Xenopus* embryogenesis (Amaya et al., 1991; Hemmati-Brivanlou and Melton, 1992). In those experiments, microinjection of mutant mRNA up to 100-fold the normal level successfully led to a targeted inactivation of specific receptor kinases. Expression of the ΔKinase epidermal growth factor RTK in *Drosophila* eyes revealed that this RTK is required for the differentiation of all cell types (Freeman, 1996). By contrast, such an approach has not been exploited widely in plants because of a few cases of cosuppression (Conner et al., 1997; Schumacher and Chory, 2000) or the inability to detect the accumulation of the transgene products (He et al., 1998). Our study demonstrated the effectiveness of the dominant-negative approach in understanding the modes of action and redundancy in the ERECTA signaling pathway.

Genetic dissection of the RLK signaling pathways that regulate plant development has been successful when the phenotypic consequences of the loss of the ligand and the receptor were nearly identical. For instance, mutations in both *CLV1* and *CLV3*, which encode an LRR-RLK and its corresponding ligand, respectively, confer identical phenotypes in meristem enlargement and increased floral organ numbers (Clark et al., 1993, 1995, 1997; Fletcher et al., 1999). Another example is the BR receptor BRI1. *bri1* was identified as a BR-insensitive mutant that displays characteristic BR-deficient phenotypes (e.g., "cabbage"-like rosettes and seedling deetiolation) (Clouse et al., 1996; Kauschmann et al., 1996; Li and Chory, 1997).

Despite the fact that RLKs constitute a large family in higher plants, with >600 members in Arabidopsis, only a handful of RLKs are known to have defined biological functions, and the identity of the corresponding ligands is far less clear (Torii, 2000; Shiu and Bleecker, 2001). It is not yet understood whether a majority of other RLKs possess modes of action similar to that of ERECTA or whether their ΔKinase fragments retain partial activity to transduce signals. In any event, the truncated receptor kinase system established in this study could serve as a powerful, alternative tool to elucidate the biological functions and signaling components of other RLKs, whose single loss-of-function mutations may not give any phenotypes as a result of complex redundancy.

METHODS

Plant Materials and Growth Conditions

Arabidopsis thaliana ecotype Columbia was used as the wild type. *erecta-103* and *erecta-105* were backcrossed four times into the wild type before use (Torii et al., 1996). Plants were grown on soil mixture (Sunshine Mix4:vermiculite:perlite, 2:1:1, Sun Gro Horticulture Canada,

Seba Beach, Canada) supplemented with 0.85 mg/cm^3 Osmocoat 14-14-14 (Scotts, Maysville, OH) under an 18-h-light/6-h-dark cycle at 21°C.

Generation of Transgenic Plants Expressing ΔKinase

To construct the plasmid carrying the truncated ERECTA, we introduced the stop codon behind the putative transmembrane domain at amino acid position 615 by PCR. PCR was performed using pKUT196, which contains the entire *ERECTA* locus from Columbia, as a template and primers Erg5858link (5′-ATGAATTCTGTCTGCAGTGTCAATCTCTA-3′) and ER6000Bam.rc (5′-TCAGGATCCTATGATCCATCAAGAAAAGGAGG-3′). The amplified fragment was digested with PstI and BamHI and introduced into plasmid pKUT197 to generate pESH101. The EcoRI-BamHI fragment of pESH101, which contains the 1.7-kb *ERECTA* promoter and the coding region of the truncated ERECTA, was cloned into pKUT531, a pPZP222-based binary vector, which contains the 1.9-kb *ERECTA* terminator (Hajdukiewicz et al., 1994). The plasmid was named pESH201.

To generate the *ΔKinase–c-Myc* construct, the following cloning steps were performed. To introduce the BamHI site after Ser-615 of *ERECTA*, PCR was performed using pKUT196 as a template and primers Erg5868link (5′-ATGAATTCTGTCTGCAGTGTCAATCTCTA-3′) and ER-6000link.rc (5′-TCAGGATCCGCTGATCCATCAAGAAAAGGAGG-3′). The amplified fragment was cloned into PstI-BamHI–digested pKUT197 to generate pESH113. The triple c-Myc sequence was amplified by PCR using primers myc-5 (5′-GAAGATCTCGAGTTCGGTGAACAAAAGTT-3′) and myc-3 (5′-CGGGATCCTTACCCTAGCTTTCCGTTCAAGT-3′) with pSLJ13471 as a template (Jones et al., 1992). The amplified fragment was digested with BglII and BamHI and inserted into BamHI-digested pESH113. The resulting plasmid, pESH115, contains the additional sequence 5′-ADLEFG(EQKLISEEDLNG)$_3$KLG-3′ after Ser-615 of ERECTA. EcoRI-BamHI–digested pESH115 was cloned into pKUT531 to generate pESH215.

To generate ΔKinase$_{M282I}$, PCR was performed using *erecta-103* genomic DNA as a template with primers ERg1761 (5′-GTATATCTAAAAACGCAGTCG-3′) and ERg2339rc (5′-CAACAACATTGAAGGTGACATTTT-3′). The amplified fragment was digested with SpeI and SacI and replaced the SpeI-SacI fragment of pESH101. The resulting plasmid, pKUT572.3, was digested with AflII and SacI and inserted into pESH201 to generate pKUT574.3. The sequences of all fragments created by PCR were confirmed. pESH201, pESH215, and pKUT574.3 were introduced into *Agrobacterium tumefaciens* strain GV3101/pMP90 by electroporation and into Arabidopsis wild-type and *erecta-105* plants using the vacuum infiltration method (Bechtold et al., 1993).

Scanning Electron Microscopy

Tissue samples were fixed overnight in 4% (v/v) glutaraldehyde in 25 mM $NaPO_4$ buffer, pH 7.0, and subsequently with 1% osmium tetroxide in 25 mM $NaPO_4$ buffer for 4 to 5 days at 4°C. The samples were dehydrated with a graded series of ethanol, critical point dried, sputter coated with gold, and observed with a scanning electron microscope (JEOL 840A).

Light Microscopy

Tissue samples were fixed overnight in 4% (v/v) paraformaldehyde in 25 mM $NaPO_4$ buffer, pH 7.0, at 4°C, dehydrated with a graded series of ethanol, and infiltrated with polymethacryl resin Technovit 7100 (Heraeus Kulzer, Wehrheim, Germany) followed by embedding and polymerization in Technovit 7100. Nine-micrometer sections were prepared using a Leica RM-6145 microtome (Wetzlar, Germany). The tissue sections were stained with 0.1% toluidine blue in 0.1 M $NaPO_4$ buffer, pH 7.0, and observed under bright-field illumination.

Antiserum Production and Purification

The cDNA sequence encoding the extracellular domain of ERECTA (ER-LRR; amino acids 36 to 577) was amplified using primers ERLRRab5 (5′-CGGAATTCTCATTCAAAGATGTGAACAATG-3′) and ERLRRab3 (5′-CGTCTAGACTATGACACTCGTACAGTTCGA-3′), with pKUT161 as a template (Torii et al., 1996). The amplified fragment was inserted in the EcoRI-XbaI–digested modified pSP73ΔAatII vector (Promega) to generate pKUT534. The sequence was confirmed. Subsequently, the fragment was inserted in pMal-c2 vector (New England Biolabs, Beverly, MA) and pGEX4T-1 vector (Amersham Pharmacia Biotech) to generate pKUT535 (maltose binding protein [MBP]-ERLRR) and pKUT538 (glutathione *S*-transferase [GST]-ERLRR), respectively. The fusion proteins were expressed in *Escherichia coli* BL21/DE3(pLysS). The inclusion bodies of *E. coli* expressing MBP-ERLRR were separated by SDS-PAGE, and the recombinant protein was excised from the gel. Polyclonal ER-LRR antisera were raised in rabbits at Cocalico Biologicals (Reamstown, PA). Affinity purification of antibodies was performed using the GST-ERLRR fusion protein immobilized on nitrocellulose membranes.

Protein Gel Blot and Immunoblot Analyses

One gram of Arabidopsis bud clusters (inflorescence tips) was ground in liquid nitrogen, mixed with 2 mL of ice-cold lysis buffer (50 mM Tris, pH 7.5, 1 mM EDTA, 100 mM NaCl, 0.1% SDS, 0.1% Triton X-100, 0.7% β-mercaptoethanol, and 1 mM phenylmethylsulfonyl fluoride) and 0.5 mL of loading buffer (200 mM Tris-HCl, pH 6.8, 8% SDS, 0.4% bromphenol blue, 40% glycerol, and 10% β-mercaptoethanol), and boiled for 5 min. Proteins were separated by 8% SDS-PAGE. SeeBlue prestained protein standards (Invitrogen, Carlsbad, CA) were used as molecular mass markers. For visualization of the total proteins, the gel was stained with Coomassie Brilliant Blue R250. For immunoblot analysis, the proteins were transferred from the gel to Hybond enhanced chemiluminescence nitrocellulose membranes (Amersham Pharmacia Biotech) using a semidry blotting apparatus (Owl Separation Systems, Portsmouth, NH). The membranes were blocked with 5% BSA in PBS for 2 h at room temperature and probed with primary antibody at a dilution of 1:15 for the affinity-purified ERLRR polyclonal antibody or 1:600 for the 9E10 anti-c-Myc monoclonal antibody (Covance, Richmond, CA) in PBS with 1% BSA at 4°C overnight. Goat anti-rabbit and sheep anti-mouse horseradish peroxidase–linked antibodies were used as secondary anti-ERLRR and anti-c-Myc antibodies, respectively, at a dilution of 1:35,000 in 0.1% Tween 20/PBS for 1 h at room temperature. The detection of ERECTA, ΔKinase, and ΔKinase–c-Myc was performed with the Chemiluminescence assay kit (Amersham Pharmacia Biotech).

Reverse Transcriptase–Mediated PCR

Total RNA was isolated from Arabidopsis bud clusters using the RNeasy Plant Mini Kit (Qiagen, Valencia, CA) and treated with DNaseI Amp grade (Gibco BRL). First-strand cDNA was synthesized from 2 μg of RNA with random hexamer primers using the ThermoScript reverse transcriptase–mediated PCR system (Gibco BRL) according to the manufacturer's instructions. PCR was performed with 0.5 μL of the first-strand reaction at 96°C for 2 min, then with varying numbers of cycles at 96°C for 35 s, 60°C for 45 s, 72°C for 90 s, and then at 72°C for 10 min. The primers ERK7 (5′-CACAGAGACGTGAAGTCGT-3′) and ERg7361rc (5′-AGCTTAACGCAACGAAAAGATACC-3′) were used to amplify endogenous *ERECTA*. The primers ERg5022 (5′-CTTGAGTAGAAATCATATAACT-3′) and ERg5757rc (5′-TGACACGGTGAGTTTAGCCAA-3′) were used to simultaneously amplify both the endogenous *ERECTA* and the introduced *ΔKinase*. The primers ERg5022 (5′-CTTGAGTAGAAATCATATAACT-3′) and ERg7361.rc (5′-AGCTTAACGCAACGAAAAGATACC-3′) were used

to amplify the introduced *ΔKinase*. Transcripts of the actin gene were amplified as a control using primers ACT2-1 (5′-GCCATCCAAGCTGTTCTCTC-3′) and ACT2-2 (5′-GCTCGTAGTCAACAGCAACAA-3′). *WUS* transcripts were amplified as described by Hamada et al. (2000). Reverse transcriptase–mediated PCR products were electrophoresed on agarose gels and visualized by staining with ethidium bromide.

Far-Western Analysis of the ERECTA–KAPP Interaction

For protein-protein interaction (far-western) blot analysis, the kinase domains of ERECTA and RLK5 were expressed as MBP fusions. The ERECTA kinase domain (corresponding to amino acids 611 to 977) was amplified from cDNA using the primers ERK4 (5′-CGGAATTCACTAGTACCATGGACAAACCAGTAACTTATTCG-3′) and ER3rc (5′-CGGGATCCACTAGTGCATAATACTTTACATGAGA-3′). The amplified fragment was digested with EcoRI and BamHI and introduced into pSP73ΔAatII to generate pKUT503. To make a kinase-inactive version of ERECTA, the invariant Lys (Lys-676) was replaced with a Glu. The first round of PCR was performed with the primer pairs ERK4 and ERKI3/K676E (5′-CTGTGGGTTGTGAGAGTAAAGCCGTTCAATCGCAACCG-3′) and ERKI5/K676E (5′-TTGAACGGCTTTACTCTCACAACCCA-3′) and ERCodeC3 (5′-CGGGATCCACTAGTCTACTCACTGTTCTGAGAAATAACTT-3′). In the next round, products from both reactions were mixed and amplified with ERK4 and ERCodeC3. The amplified fragment was digested with EcoRI and BamHI and introduced into the plasmid pSP73ΔAatII to generate pKUT536. The EcoRI-SalI fragments of both pKUT503 and pKUT536 were cloned into pMAL-c2 (New England Biolabs). The plasmids RLK5CAT-MBP, RLK5CAT(K711E)MBP, and GST-KID134 were generous gifts from John Walker (University of Missouri, Columbia).

The recombinant MBP and GST fusion proteins were expressed in *E. coli* strain AD494/DE3 and purified by affinity chromatography on amylose-agarose resin (New England Biolabs) or glutathione–Sepharose 4B resin (Amersham Pharmacia Biotech), respectively, according to the manufacturers' instructions. GST-KID was labeled with ^{32}P as described (Braun et al., 1997). Protein concentrations were determined with Bio-Rad Protein Assay Solution. One milligram each of ERCAT-MBP, ERCAT(K676E)-MBP, RLK5CAT-MBP, and RLK5CAT(K711E)-MBP was blotted onto a Hybond enhanced chemiluminescence nitrocellulose membrane (Amersham Pharmacia Biotech), and far-western analysis with radiolabeled KID protein was performed according to Braun et al. (1997).

Gel Filtration Analysis

The Arabidopsis bud clusters were ground in liquid nitrogen, mixed with 2 volumes of ice-cold extraction buffer (50 mM Hepes, pH 7.4, 10 mM EDTA, 1% Triton X-100, and 1% protease inhibitor cocktail [Sigma]), filtered through Miracloth (Calbiochem), and centrifuged at 1500*g* for 10 min at 4°C. The supernatant was ultracentrifuged subsequently at 100,000*g* for 1 h at 4°C. Membrane proteins from *ERECTA*::*ΔKinase–c-Myc/ercta-105* bud clusters were isolated in a similar manner except that no Triton X-100 was added to the extraction buffer and pellet instead of supernatant was recovered. Subsequently, the pellet was resuspended in extraction buffer containing 1% Triton X-100, and the supernatant was used for chromatography. Gel filtration was performed using a fast protein liquid chromatography system (Amersham Pharmacia Biotech) with a Superose 6 HR10/30 column (Amersham Pharmacia Biotech) at a flow rate of 0.4 mL/min. Column equilibration and chromatography were performed in the following buffer: 0.05 mM $NaPO_4$, pH 7.3, 0.05 mM NaCl, 0.02% Na azide, and 1% Triton X-100. Next, 0.2-mL fractions were collected and concentrated by incubation with trichloroacetic acid (20% final concentration) for 30 min on ice and subsequent centrifugation at 13,500 rpm for 10 min at 4°C. The precipitates were washed with acetone, vacuum-dried, and resuspended in 20 μL of loading buffer. Concentrated fractions were subjected to immunoblotting and probed with either anti-c-Myc or anti-ERECTA LRR antibodies as described above. High and low molecular mass gel-filtration calibration kits (Amersham Pharmacia Biotech) were used as molecular mass standards.

Flow Cytometry

For flow cytometric analysis of Arabidopsis nuclear DNA content, 50 to 100 mg of mature pedicel tissues was collected from 4- to 6-week-old plants. To ensure the uniformity of the samples, pedicels bearing flower buds, flowers, youngest five siliques, and siliques turning yellow were discarded. The pedicel samples were chopped finely in 1.5 mL of the ice-cold extraction buffer (15 mM Hepes, 1 mM EDTA, 80 mM KCl, 20 mM NaCl, 300 mM sucrose, 0.2% Triton X-100, 0.5 mM spermine, and 0.1% β-mercaptoethanol) for 3 min, passed through the filter, and centrifuged at 13,000 rpm for 1 min. The pellet was resuspended with 650 mL of the staining buffer (0.1 mg/mL propidium iodide and 100 μg/mL RNase A in the extraction buffer), passed through the filter, and subjected to analysis using FACSI (Becton-Dickinson, Franklin Lakes, NJ) at the Cell Analysis Facility (Department of Immunology, University of Washington). For each measurement, 50,000 events were recorded at 560 V of the FL2 channel. At least two independent extractions were performed for each genotype, and two or three independent measurements were performed for each extraction.

Upon request, all novel materials described in this article will be made available in a timely manner for noncommercial research purposes.

ACKNOWLEDGMENTS

We thank Tatsuo Kakimoto, Zhenbiao Yang, Chris Berthiaume, and Emi Hill for commenting on the manuscript; Phil Soriano for valuable discussion about the modes of action of animal receptor kinases; Susana Rivas and Jonathan Jones for providing pSLJ13741; Kevin Lease, Jia Li, and John Walker for the gift of RLK5CAT-MBP, RLK5CAT(K711E)MBP, and GST-KID134; Jerry Davison and Kim Young for assistance with flow cytometry; and Sungha Kim for technical assistance. K.U.T. thanks Steve Clark for support during her career transition. This work was supported in part by the start-up fund and Royalty Research Fund Grant 2499 from the University of Washington and by a CREST award from the Japan Science and Technology Corporation to K.U.T.

Received January 9, 2003; accepted February 23, 2003.

REFERENCES

Amaya, E., Musci, T., and Kirschner, M. (1991). Expression of a dominant-negative mutant of the FGF receptor disrupts mesoderm formation in Xenopus embryos. Cell **66,** 257–270.

Ataliotis, P., and Mercola, M. (1997). Distribution and function of platelet-derived growth factors and their receptors during embryogenesis. Int. Rev. Cytol. **172,** 95–125.

Azpiroz, R., Wu, Y., LoCascio, J.C., and Feldmann, K.A. (1998). An Arabidopsis brassinosteroid-dependent mutant is blocked in cell elongation. Plant Cell **10,** 219–230.

Bechtold, N., Ellis, J.G., and Pelletier, G. (1993). *In planta Agrobacterium*-mediated gene transfer by infiltration of adult *Arabidopsis thaliana* plants. C. R. Acad. Sci. Paris **316,** 1194–1199.

Beguinot, L., Lyall, R., Willingham, M., and Pastan, I. (1984). Down-regulation of the epidermal growth factor receptor in KB cells is due

to receptor internalization and subsequent degradation in lysosomes. Proc. Natl. Acad. Sci. USA **81,** 2384–2388.

Bowman, J.L. (1993). Arabidopsis: An Atlas of Morphology and Development. (New York: Springer-Verlag).

Brand, U., Fletcher, J., Hobe, M., Meyerowitz, E., and Simon, R. (2000). Dependence of stem cell fate in Arabidopsis on a feedback loop regulated by CLV3 activity. Science **289,** 617–619.

Braun, D.M., Stone, J.M., and Walker, J.C. (1997). Interaction of the maize and *Arabidopsis* kinase interaction domains with a subset of receptor-like protein kinases: Implications for transmembrane signaling in plants. Plant J. **12,** 83–95.

Clark, S.E., Running, M.P., and Meyerowitz, E.M. (1993). *CLAVATA1*, a regulator of meristem and flower development in *Arabidopsis*. Development **119,** 397–418.

Clark, S.E., Running, M.P., and Meyerowitz, E.M. (1995). *CLAVATA3* is a specific regulator of shoot and floral meristem development affecting the same processes as *CLAVATA1*. Development **121,** 2057–2067.

Clark, S.E., Williams, R.W., and Meyerowitz, E.M. (1997). The *CLAVATA1* gene encodes a putative receptor kinase that controls shoot and floral meristem size in Arabidopsis. Cell **89,** 575–585.

Clouse, S., Langford, M., and McMorris, T. (1996). A brassinosteroid-insensitive mutant in *Arabidopsis thaliana* exhibits multiple defects in growth and development. Plant Physiol. **111,** 671–678.

Conner, J., Tantikanjana, T., Stein, J., Kandasamy, M., Nasrallah, J., and Nasrallah, M. (1997). Transgene-induced silencing of *S*-locus genes and related genes in *Brassica*. Plant J. **11,** 809–823.

De Veylder, L., Beeckman, T., Beemster, G.T., Krols, L., Terras, F., Landrieu, I., van der Schueren, E., Maes, S., Naudts, M., and Inze, D. (2001). Functional analysis of cyclin-dependent kinase inhibitors of Arabidopsis. Plant Cell **13,** 1653–1668.

Fletcher, J.C., Brand, U., Running, M.P., Simon, R., and Meyerowitz, E.M. (1999). Signaling of cell fate decisions by *CLAVATA3* in *Arabidopsis* shoot meristems. Science **283,** 1911–1914.

Freeman, M. (1996). Reiterative use of the EGF receptor triggers differentiation of all cell types in the Drosophila eye. Cell **87,** 651–660.

Fridborg, I., Kuusk, S., Moritz, T., and Sundberg, E. (1999). The Arabidopsis dwarf mutant *shi* exhibits reduced gibberellin responses conferred by overexpression of a new putative zinc finger protein. Plant Cell **11,** 1019–1032.

Givol, D., and Yayon, A. (1992). Complexity of FGF receptors: Genetic basis for structural diversity and functional specificity. FASEB J. **6,** 3362–3369.

Hajdukiewicz, P., Svab, Z., and Maliga, P. (1994). The small, versatile pPZP family of Agrobacterium binary vectors for plant transformation. Plant Mol. Biol. **25,** 989–994.

Hamada, S., Onouchi, H., Tanaka, H., Kudo, M., Liu, Y.G., Shibata, D., Machida, C., and Machida, Y. (2000). Mutations in the WUSCHEL gene of *Arabidopsis thaliana* result in the development of shoots without juvenile leaves. Plant J. **24,** 91–101.

He, Z.-H., He, D., and Kohorn, B.D. (1998). Requirement for the induced expression of a cell wall associated receptor kinase for survival during the pathogen response. Plant J. **14,** 55–63.

Hemmati-Brivanlou, A., and Melton, D. (1992). A truncated activin receptor inhibits mesoderm induction and formation of axial structures in Xenopus embryos. Nature **359,** 609–614.

Jeong, S., Trotochaud, A.E., and Clark, S.E. (1999). The Arabidopsis CLAVATA2 gene encodes a receptor-like protein required for the stability of the CLAVATA1 receptor-like kinase. Plant Cell **11,** 1925–1933.

Jinn, T.L., Stone, J.M., and Walker, J.C. (2000). HAESA, an *Arabidopsis* leucine-rich repeat receptor kinase, controls floral organ abscission. Genes Dev. **11,** 108–117.

Jones, J.D., Shlumukov, L., Carland, F., English, J., Scofield, S.R., Bishop, G.J., and Harrison, K. (1992). Effective vectors for transformation, expression of heterologous genes, and assaying transposon excision in transgenic plants. Transgenic Res. **1,** 285–297.

Jones, S., Foreman, S., Shank, B., and Kurten, R. (2002). EGF receptor downregulation depends on a trafficking motif in the distal tyrosine kinase domain. Am. J. Physiol. Cell Physiol. **282,** C420–C433.

Kauschmann, A., Jessop, A., Koncz, C., Szekeres, M., Willmitzer, L., and Altmann, T. (1996). Genetic evidence for an essential role of brassinosteroids in plant development. Plant J. **9,** 701–713.

Komeda, Y., Takahashi, T., and Hanzawa, Y. (1998). Development of inflorescences in *Arabidopsis thaliana*. J. Plant Res. **111,** 283–288.

Kondorosi, E., Roudier, F., and Gendreau, E. (2000). Plant cell size control: Growing by ploidy? Curr. Opin. Plant Biol. **3,** 488–492.

Lease, K.A., Lau, N.Y., Schuster, R.A., Torii, K.U., and Walker, J.C. (2001a). Receptor serine/threonine protein kinases in signaling: Analysis of the ERECTA receptor-like kinase of *Arabidopsis thaliana*. New Phytol. **151,** 133–144.

Lease, K.A., Wen, J., Li, J., Doke, J.T., Liscum, E., and Walker, J.C. (2001b). A mutant Arabidopsis heterotrimeric G-protein beta subunit affects leaf, flower, and fruit development. Plant Cell **13,** 2631–2641.

Leyser, H., and Furner, I. (1992). Characterization of 3 shoot apical meristem mutants of *Arabidopsis thaliana*. Development **116,** 397–403.

Li, J., and Chory, J. (1997). A putative leucine-rich repeat receptor kinase involved in brassinosteroid signal transduction. Cell **90,** 929–938.

Li, J., Wen, J., Lease, K.A., Doke, J.T., Tax, F.E., and Walker, J.C. (2002). BAK1, an Arabidopsis LRR receptor-like protein kinase, interacts with BRI1 and modulates brassinosteroid signaling. Cell **110,** 213–222.

Li, X., et al. (2000). PDGF-C is a new protease-activated ligand for the PDGF α-receptor. Nat. Cell Biol. **2,** 302–309.

Matsubayashi, Y., Ogawa, M., Morita, A., and Sakagami, Y. (2002). An LRR receptor kinase involved in perception of a peptide plant hormone, phytosulfokine. Science **296,** 1470–1472.

Nam, K.H., and Li, J. (2002). BRI1/BAK1, a receptor kinase pair mediating brassinosteroid signaling. Cell **110,** 203–212.

Piedras, P., Rivas, S., Droge, S., Hillmer, S., and Jones, J. (2000). Functional, c-myc-tagged Cf-9 resistance gene products are plasma-membrane localized and glycosylated. Plant J. **21,** 529–536.

Rivas, S., Mucyn, T., van den Berg, H., Vervoort, J., and Jones, J. (2002a). An $\sim$400 kDa membrane-associated complex that contains one molecule of the resistance protein Cf-4. Plant J. **29,** 783–796.

Rivas, S., Romeis, T., and Jones, J.D. (2002b). The Cf-9 disease resistance protein is present in an approximately 420-kilodalton heteromultimeric membrane-associated complex at one molecule per complex. Plant Cell **14,** 689–702.

Schoof, H., Lenhard, M., Haecker, A., Mayer, K., Jürgens, G., and Laux, T. (2000). The stem cell population of Arabidopsis shoot meristem is maintained by a regulatory loop between the *CLAVATA* and *WUSCHEL* genes. Cell **100,** 635–644.

Schumacher, K., and Chory, J. (2000). Brassinosteroid signal transduction: Still casting the actors. Curr. Opin. Plant Biol. **3,** 79–84.

Shiu, S.H., and Bleecker, A.B. (2001). Receptor-like kinases from Arabidopsis form a monophyletic gene family related to animal receptor kinases. Proc. Natl. Acad. Sci. USA **98,** 10763–10768.

Stone, J.M., Collinge, M.A., Smith, R.D., Horn, M.A., and Walker, J.C. (1994). Interaction of a protein phosphatase with an *Arabidopsis* serine/threonine receptor kinase. Science **266,** 793–795.

Stone, J.M., Trotochaud, A.E., Walker, J.C., and Clark, S.E. (1998). Control of meristem development by CLAVATA1 receptor kinase and kinase-associated protein phosphatase interactions. Plant Physiol. **117,** 1217–1225.

Szekeres, M., Nemeth, K., Koncz-Kalman, Z., Mathur, J., Kauschmann, A., Altmann, T., Redei, G.P., Nagy, F., Schell, J., and Koncz, C.

(1996). Brassinosteroids rescue the deficiency of CYP90, a cytochrome P450, controlling cell elongation and deetiolation in *Arabidopsis*. Cell **85,** 171–182.

Timpte, C., Wilson, A., and Estelle, M. (1992). Effects of the *axr2* mutation of Arabidopsis on cell-shape in hypocotyl and inflorescence. Planta **188,** 271–278.

Torii, K.U. (2000). Receptor kinase activation and signal transduction in plants: An emerging picture. Curr. Opin. Plant Biol. **3,** 361–367.

Torii, K.U., Mitsukawa, N., Oosumi, T., Matsuura, Y., Yokoyama, R., Whittier, R.F., and Komeda, Y. (1996). The Arabidopsis *ERECTA* gene encodes a putative receptor protein kinase with extracellular leucine-rich repeats. Plant Cell **8,** 735–746.

Trotochaud, A.E., Hao, T., Wu, G., Yang, Z., and Clark, S.E. (1999). The Arabidopsis CLV1 receptor-like kinase requires CLV3 for its assembly into a signaling complex that includes KAPP and a Rho GTPase. Plant Cell **11,** 393–405.

Ueno, H., Colbert, H., Escobedo, J.A., and Williams, L.T. (1991). Inhibition of PDGF β receptor signal transduction by coexpression of a truncated receptor. Science **252,** 844–847.

Ueno, H., Escobedo, J.A., and Williams, L.T. (1993). Dominant-negative mutations of platelet-derived growth factor (PDGF) receptors: Inhibition of receptor function by ligand-dependent formation of heterodimers between PDGF α- and β-receptors. J. Biol. Chem. **268,** 22814–22819.

Wang, G.-L., et al. (1998). *Xa21D* encodes a receptor-like molecule with a leucine-rich repeat domain that determines race-specific recognition and is subjected to adaptive evolution. Plant Cell **10,** 765–779.

Wang, H., Zhou, Y., Gilmer, S., Whitwill, S., and Fowke, L.C. (2000). Expression of the plant cyclin-dependent kinase inhibitor ICK1 affects cell division, plant growth and morphology. Plant J. **24,** 613–623.

Williams, R.W., Wilson, J.M., and Meyerowitz, E.M. (1997). A possible role for kinase-associated protein phosphatase in the *Arabidopsis* CLAVATA1 signaling pathway. Proc. Natl. Acad. Sci. USA **94,** 10467–10472.

Yokoyama, R., Takahashi, T., Kato, A., Torii, K.U., and Komeda, Y. (1998). The Arabidopsis *ERECTA* gene is expressed in the shoot apical meristem and organ primordia. Plant J. **15,** 301–310.

Yu, L.P., Simon, E.J., Trotochaud, A.E., and Clark, S.E. (2000). *POLTERGEIST* functions to regulate meristem development downstream of the *CLAVATA* loci. Development **127,** 1661–1670.